

Supporting Information (SI)

Triplet 4-Nitrenemethyl-Pyridine-*N*-Oxide: A Model Alkyl Nitrene Isolated in Cryogenic Matrices

Cláudio M. Nunes,^{1*} A. J. Lopes Jesus,² Tatiana Caneca,¹ Gemma Aragay,³ Pablo Ballester,^{3,4} and Rui Fausto^{1,4}

¹University of Coimbra, CQC-IMS, Department of Chemistry, 3004-535 Coimbra, Portugal

²University of Coimbra, CQC-IMS, Faculty of Pharmacy, 3004-295 Coimbra, Portugal

³Institute of Chemical Research of Catalonia (ICIQ), The Barcelona Institute of Science and Technology (BIST), 43007 Tarragona, Spain

⁴ICREA, Passeig Lluís Companys 23, 08018 Barcelona, Spain

⁵Spectroscopy@IKU, Faculty Sciences and Letters, Department of Physics, Istanbul Kultur University, Bakirkoy, Istanbul 34158, Turkey

TABLE OF CONTENTS

1. FIGURES	S2
2. TABLES	S6
3. COMPUTATIONAL DATA	S7

1. FIGURES

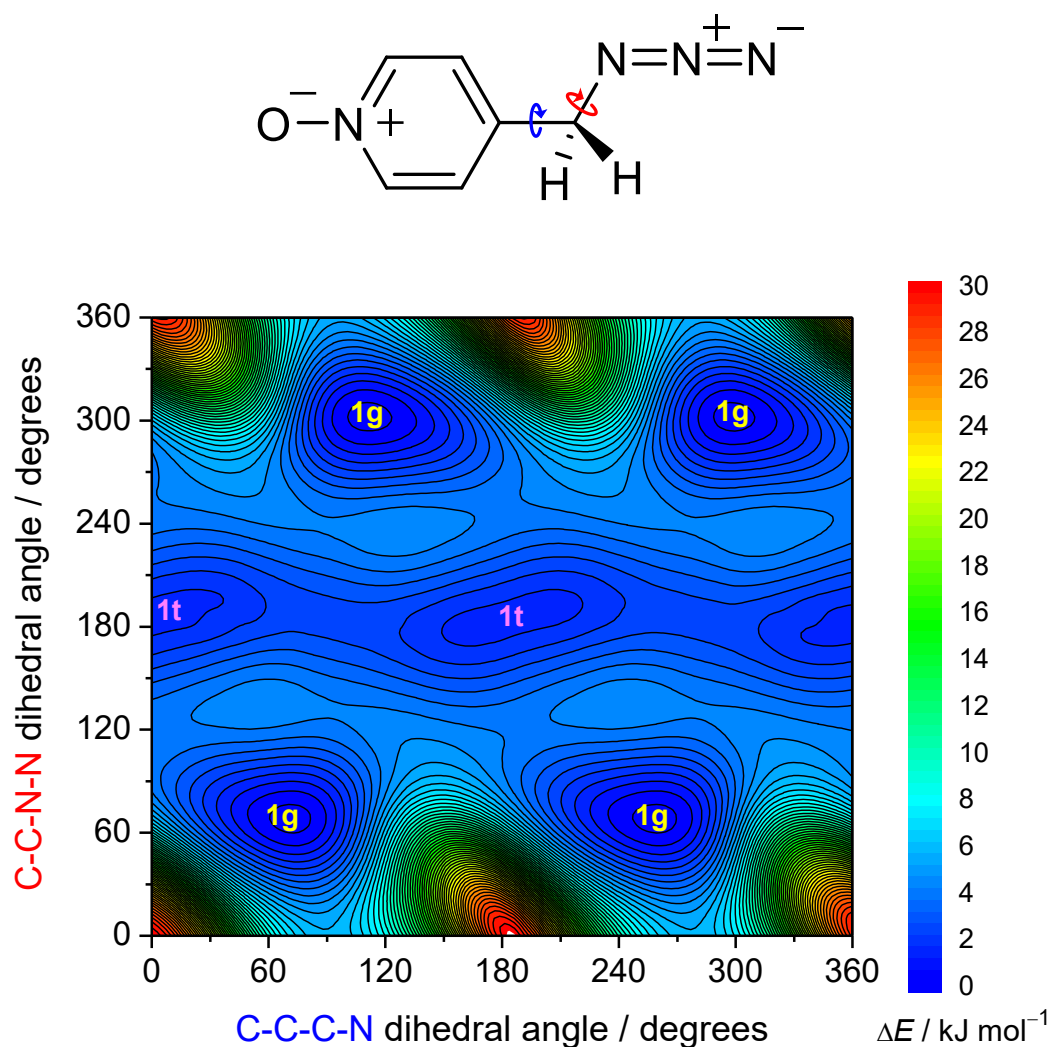


Figure S1. Two-dimensional map of the potential energy of 4-azidomethyl-pyridine-*N*-oxide **1** as a function of the C-C-C-N and C-C-N-N dihedral angles. Each dihedral was incremented by 10°, with all remaining structural parameters fully optimized at the B3LYP/6-311+G(2d,p) level. Energy minima are denoted as **1g** (fourfold degenerate) and **1t** (doubly degenerate). The color scale corresponds to relative energies, referenced to the lowest minimum (**1g**), and isoenergy lines are drawn every 1 kJ mol⁻¹.

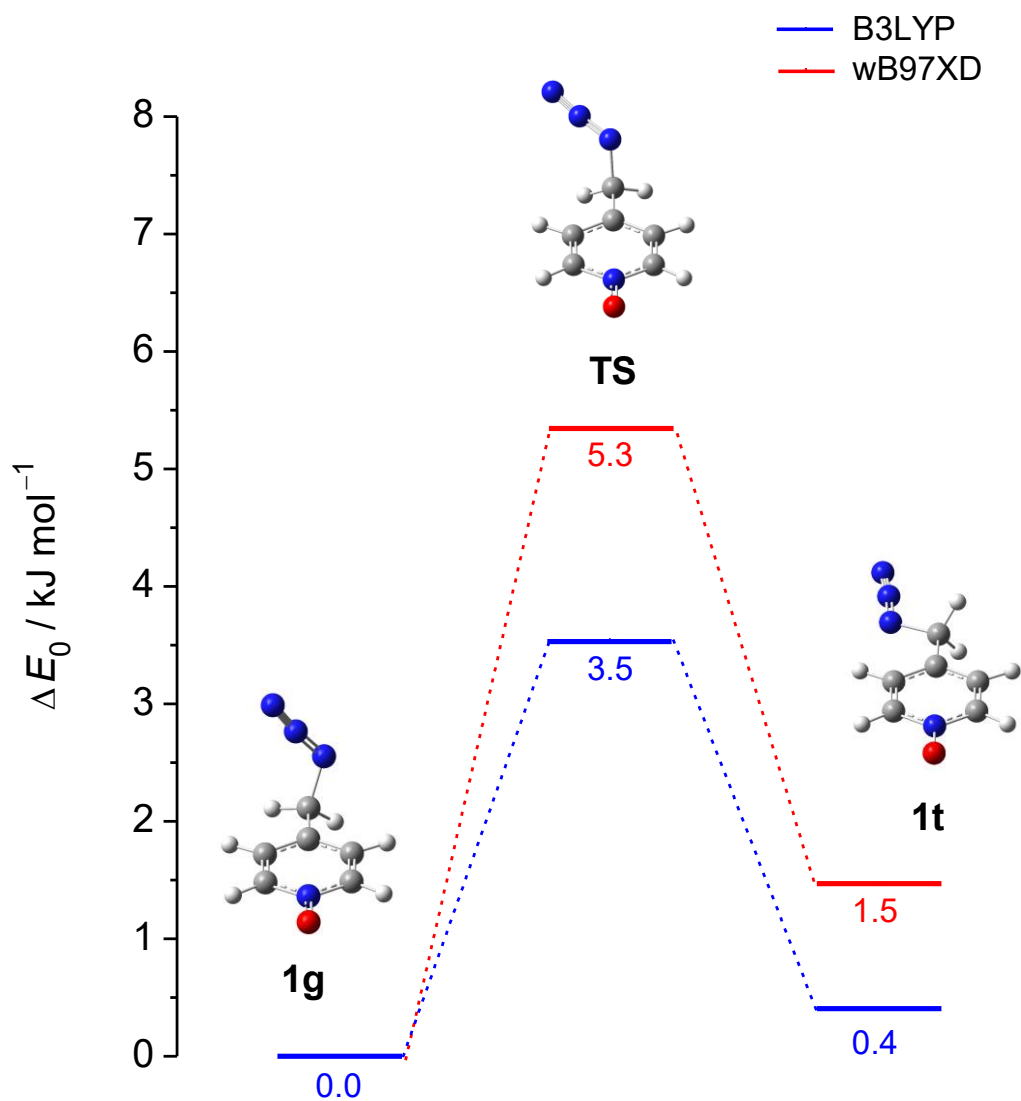


Figure S2. Potential-energy diagram showing the relative zero-point-corrected energies of the **1g** and **1t** conformers of 4-azidomethyl-pyridine-*N*-oxide **1**, together with the transition state along the minimum-energy path connecting the two conformers. The energy of the most stable conformer (**1g**) was taken as the zero of the relative energy scale. The energies shown were computed at the B3LYP/6-311+G(2d,p) (blue) and ω B97XD/6-311+G(2d,p) (red) levels of theory.

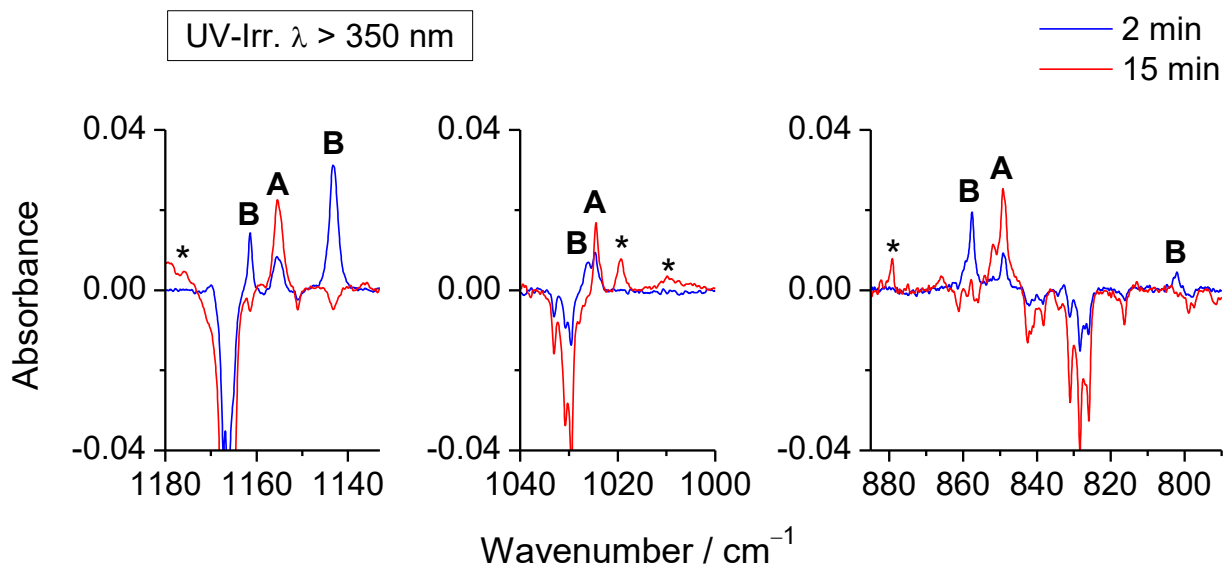


Figure S3. Experimental IR difference spectra showing the spectral changes observed after 2 min of UV irradiation ($\lambda \geq 350$ nm), followed by an additional 13 min of irradiation (15 min total) under identical conditions, of 4-azidomethyl-pyridine-*N*-oxide **1** isolated in an Ar matrix at 15 K. Positive and negative bands correspond to photogenerated and consumed species, respectively. The spectral changes indicate that the primary photoproducts **A** (assigned to triplet 4-nitrenemethyl-pyridine-*N*-oxide **3****2**) and **B** (assigned to 4-iminomethyl-pyridine-*N*-oxide **3**) are both formed within the first 2 minutes of irradiation. Upon prolonged irradiation, **B** is consumed concomitantly with **1**, whereas **A** continues to accumulate in the matrix. Bands marked with an asterisk are assigned unidentified secondary photoproducts.

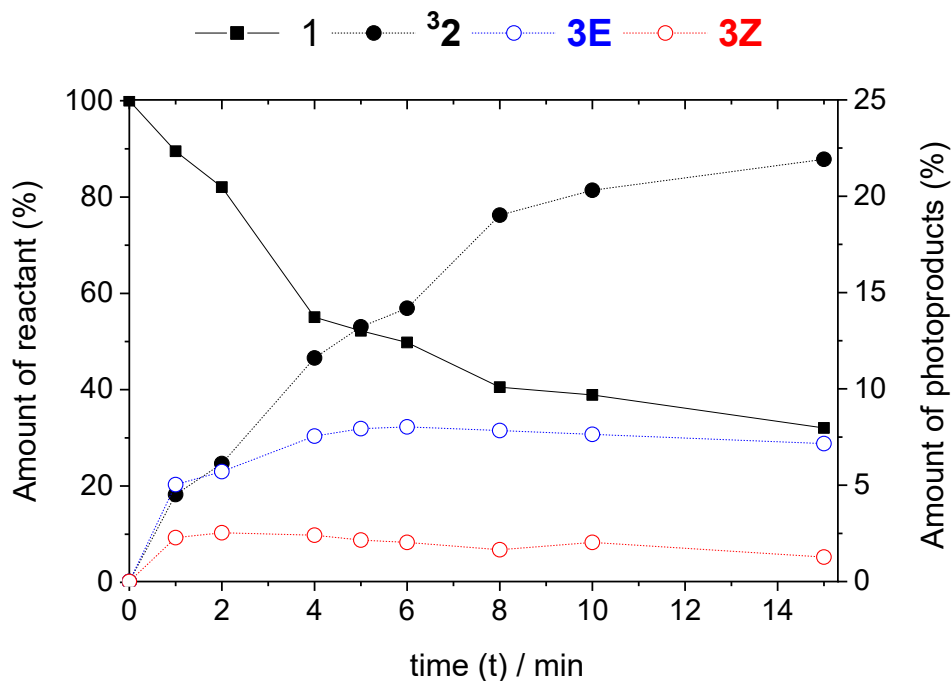


Figure S4. Time evolution of the amounts of 4-azidomethyl-pyridine-*N*-oxide **1** and of its photoproducts 4-nitrenemethyl-pyridine-*N*-oxide **32** and the *E*- and *Z*-isomers of 4-iminomethyl-pyridine-*N*-oxide, during UV exposure ($\lambda \geq 350$ nm) of **1** isolated in an Ar matrix at 15 K for 15 min. The relative concentrations of reactant **1** and photoproducts **32**, **3E**, and **3Z** were estimated from the integrated areas of their characteristic infrared bands. Initially, diagnostic bands were selected based on their high intensity and absence of overlap with other spectral features: 1346 cm^{-1} (**1**), 1156 cm^{-1} (**32**), 1143 cm^{-1} (**3E**), and 1161 cm^{-1} (**3Z**). To account for the different transition dipole moments of these vibrations, the experimental integrated intensities were divided by the calculated intensities of the corresponding vibrations obtained from the B3LYP/6-311+G(2d,p) calculations (see Tables 2, 3 and S1). In the final step, these weighted integrated intensities were scaled by a common normalization factor, setting the initial amount of reactant **1** at $t = 0$ min to 100%. At the early stages of photolysis ($t \leq 2$ min), the sum of all identified species remains close to 100%. At longer irradiation times, this proportion decreases to 77% at $t = 4$ min and to 62% at $t = 15$ min, reflecting the formation of additional, unidentified secondary photoproducts, which account for the remaining 23% and 38%, respectively.

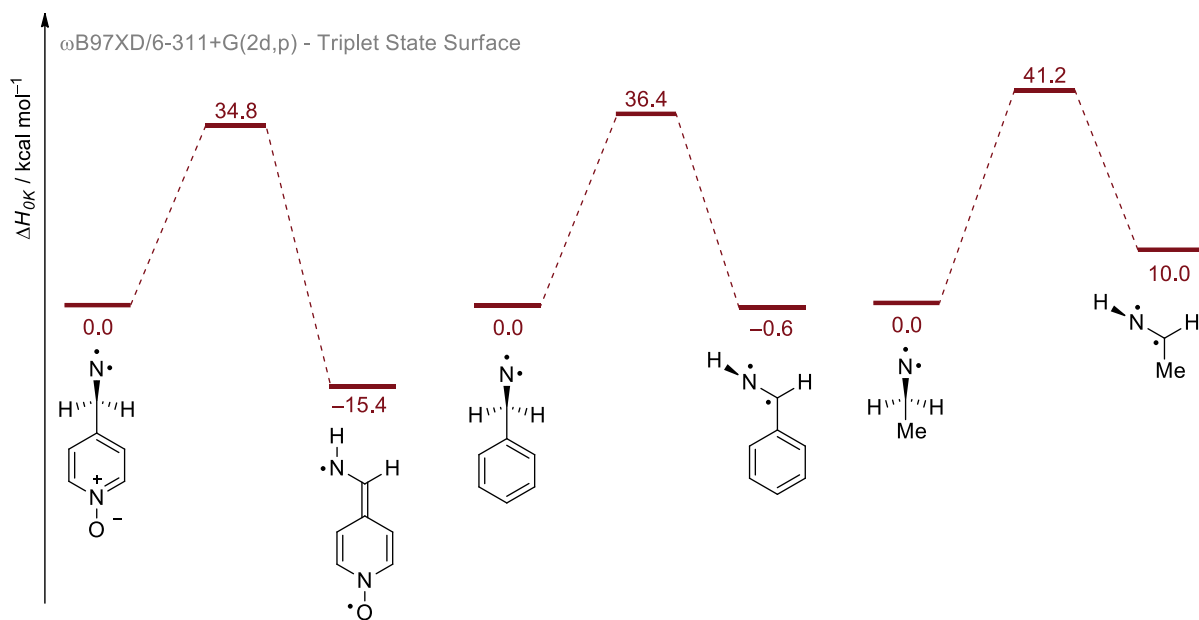


Figure S5. Reaction energy profile (ΔH_{0K} in kcal mol⁻¹) computed at the ω B97XD/6-311+G(2d,p) + ZPVE level of theory for the 1,2-H shift from triplet alkyl nitrenes to the corresponding imines. Values are relative to the energy of the corresponding triplet alkyl nitrenes

2. TABLES

Table S1. Experimental IR spectral data for azide 4-azidomethyl-pyridine-*N*-oxide **1** isolated in an Ar matrix at 15 K, compared with the B3LYP/6-311+G(2d,p) vibrational frequencies (ν , cm^{-1}) and infrared intensities (I , km mol^{-1}) calculated for the two conformers of **1** (**1g** and **1t**) and approximate vibrational assignments.^a

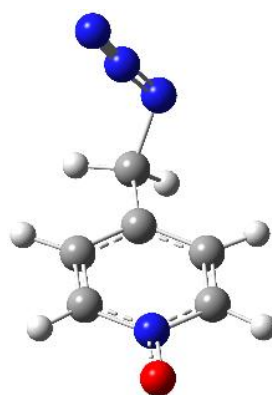
Exp. (Ar, 15 K) ^a	Calculated ^b		Conf.	Approximate assignment ^c
	$\nu_{\text{Calc.}}$	I		
2112 (vs, split)	2157.5 / 2172.9	522.2 / 745.4	1g / 1t	$\nu_{\text{as}} \text{N}_3$
1622 (m)*	1629.4 / 1633.7	38.8 / 15.3	1g / 1t	ν_{CC} ring
1547 (vw)	1534.1 / 1535.7	2.2 / 7.4	1g / 1t	[ν_{CC} ; ν_{CN}] ring
1485 (s)	1484.7 / 1486.9	107.2 / 131.1	1g / 1t	δCH ring; $\nu \text{NO} - \nu_{\text{CC}}$ exo
1459 (vw)	1465.2	8.7	1g	δCH_2
1453 (vw)	1454.2	5.0	1g	ν_{CC} ring; δCH ring
	1456.5	11.6	1t	δCH_2
1444 (w)	1449.7	17.9	1t	ν_{CC} ring; δCH ring; δCH_2
1346 (m)	1348.8 / 1351.0	9.7 / 85.7	1g / 1t	ωCH_2
1315 (m)	1305.9	91.7	1t	$\nu_s \text{N}_3$; δCH ring
1295 (s, split)	1298.7	24.0	1t	$\nu_s \text{N}_3$; δCH ring
	1300.0 / 1290.1	229.5 / 447.1	1g / 1t	νNO
1258 (m)	1265.2	179.9	1g	γCH exo; $\nu_s \text{N}_3$
1227 (w)	1233.2	37.9	1g	tw CH_2 ; $\nu_s \text{N}_3$; [νCC ; νCC] ring
1206 (vw)	1203.6	27.8	1g	νCC exo
1166 (s, split)	1172.1 / 1171.7	67.5 / 65.7	1g / 1t	δCH ring
1029 (w, split)	1026.8 / 1027.5	21.8 / 16.0	1g / 1t	δ ring
887 (vw, split)	874.1	13.4	1g	νCN exo
859 (vw, split)	856.6 / 859.4	10.1 / 4.6	1g / 1t	Ring breathing
843 (w, split)	840.3	43.1	1g	νCN exo; γCH ring; γ ring
828 (w, split)	832.2	48.6	1t	γCH ring; γ ring
816 (vw)	815.5	3.4	1t	γCH ring
799 (vw, split)	796.8	7.6	1t	δ ring; ν_{CC} exo - νNO
784 (vw)	781.0	16.2	1g	δ ring; ν_{CC} exo - νNO
663 (vw)	667.5	22.1	1g	δN_3 ; δ ring
658 (vw)	663.8	3.6	1t	δ ring
655 (vw)	659.3	3.7	1g	δ ring
629 (vw)	633.7	20.7	1t	δN_3 ; δ ring
561 (vw)	572.1 / 565.5	10.5 / 5.2	1g / 1t	γN_3
549 (vw)	548.0	20.7	1g	γ ring; γCH ring
538 (vw)	541.5	13.5	1t	δCCN exo; δ ring
510 (vw)	510.6	13.8	1t	γ ring; γCH ring
487 (vw)	491.3	19.0	1g	δ ring
476 (vw, split)	478.1 / 473.0	6.2 / 7.3	1g / 1t	δNO

^a Bands without correspondence in the calculated spectra were found at 903, 684 and 498 cm^{-1} . Experimental intensities (Int.) are expressed qualitatively: vs = very strong; s = strong; m = medium; w = weak; vw = very weak. Because of their minor relevance for the present study, absorptions bands falling in the 3000 – 2800 cm^{-1} region, which are assigned to the CH and CH_2 stretching vibrations, have not been included in this table. The band at 1622 cm^{-1} (marked with an asterisk) partially overlaps with a band at 1624 cm^{-1} , which is due to traces of monomeric water trapped in the Ar matrix. ^b Calculated harmonic wavenumbers (in cm^{-1}) were scaled by a factor of 0.979. Weak calculated vibrations without experimental counterparts and those below 400 cm^{-1} , falling outside of the spectral range covered in the KBr/DTGS setup, are omitted. ^c Approximate assignment was based on the results provided by the “vibAnalysis” software, supported by Gaussview animations. Abbreviations: ν = stretching, δ = in-plane deformation, γ = out-of-plane deformation, ω = wagging; s = symmetric, and as = antisymmetric; exo = exocyclic fragment. Sign “-” designates combinations of vibrations in the opposite phase.

3. COMPUTATIONAL DATA

Cartesian coordinates of the optimized structures are provided for all species discussed in this work, together with data from harmonic vibrational frequency calculations (scaled harmonic wavenumbers and infrared intensities) for the species detected spectroscopically. Calculated harmonic wavenumbers were scaled by factors of 0.979 below 3000 cm^{-1} and 0.960 above 3000 cm^{-1} .

4-azidomethyl-pyridine-*N*-oxide **1**, conformer **1g**



B3LYP/6-311+G(2d,p)

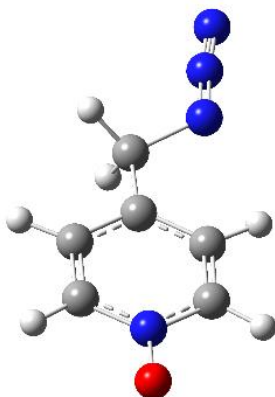
ω B97XD/6 311+G(2d,p)

6	1.649837	0.981918	0.681487	6	-1.622896	-0.909669	0.753564
6	0.363187	0.645845	1.047046	6	-0.338586	-0.561395	1.108148
6	-0.251363	-0.502106	0.551392	6	0.285649	0.540477	0.541423
6	0.499058	-1.282829	-0.331630	6	-0.444017	1.260575	-0.400440
6	1.779549	-0.926529	-0.682148	6	-1.721776	0.890488	-0.735790
1	2.178854	1.854324	1.033279	1	-2.163690	-1.751623	1.158387
1	-0.156856	1.299401	1.737338	1	0.170770	-1.170584	1.845554
1	0.082098	-2.185604	-0.761397	1	-0.012449	2.125557	-0.889656
1	2.410926	-1.486846	-1.354609	1	-2.342545	1.405248	-1.453432
7	2.368329	0.204646	-0.181203	7	-2.321067	-0.191714	-0.163473
8	3.560034	0.519711	-0.512626	8	-3.504862	-0.517046	-0.481730
6	-1.661156	-0.875941	0.926038	6	1.698960	0.919746	0.889329
1	-1.729668	-1.935091	1.168793	1	1.780151	1.991857	1.060953
1	-1.985592	-0.310771	1.804728	1	2.014362	0.411773	1.806280
7	-2.641876	-0.693515	-0.181797	7	2.661722	0.643933	-0.199179
7	-2.842980	0.471812	-0.525892	7	2.725915	-0.538079	-0.530989
7	-3.105831	1.497507	-0.922155	7	2.854614	-1.588026	-0.908023

B3LYP/6-311+G(2d,p)

$\tilde{\nu} / \text{cm}^{-1}$	I / km mol ⁻¹	$\tilde{\nu} / \text{cm}^{-1}$	I / km mol ⁻¹
3108.6	0.1	948.9	0.2
3107.4	1.1	935.7	0.6
3055.5	1.5	874.1	13.4
3051.1	3.0	856.6	10.1
2984.7	5.9	840.2	43.1
2911.8	31.6	815.1	0.2
2157.5	522.2	781.0	16.2
1629.3	38.8	718.4	6.6
1534.1	2.2	667.5	22.2
1484.7	107.2	659.3	3.7
1465.2	8.7	572.1	10.5
1454.2	5.0	548.0	20.7
1348.8	9.7	491.2	19.0
1320.3	5.8	478.2	6.2
1300.0	229.5	419.3	0.6
1265.2	179.9	374.9	2.5
1233.2	37.9	307.2	2.1
1203.5	27.8	245.9	1.0
1192.5	1.8	172.2	7.8
1172.1	67.5	105.6	4.3
1102.2	3.4	37.5	1.0
1026.8	21.8	24.8	0.9
964.0	4.2		

4-azidomethyl-pyridine-*N*-oxide **1**, conformer **1t**



B3LYP/6-311+G(2d,p)

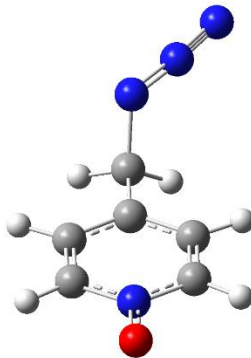
ω B97XD/6 311+G(2d,p)

6	1.745264	-1.207616	0.043422	6	-1.743209	-1.201290	0.014406
6	0.395250	-0.928396	0.075264	6	-0.393078	-0.928555	0.021595
6	-0.063075	0.385660	0.048249	6	0.063887	0.379695	0.011937
6	0.904744	1.388392	-0.016150	6	-0.898360	1.383801	-0.005440
6	2.245982	1.081571	-0.042923	6	-2.236901	1.079430	-0.010560
1	2.162263	-2.203001	0.058086	1	-2.163445	-2.195693	0.019556
1	-0.304116	-1.752272	0.113500	1	0.304284	-1.755180	0.032248
1	0.622182	2.434408	-0.048217	1	-0.613108	2.429656	-0.015203
1	3.040180	1.810468	-0.093883	1	-3.031819	1.809619	-0.024435
7	2.680794	-0.214671	-0.012050	7	-2.670353	-0.210525	-0.001523
8	3.930340	-0.486207	-0.039605	8	-3.913502	-0.476156	-0.009003
6	-1.523524	0.749615	0.118561	6	1.523605	0.744504	0.031069
1	-1.764827	1.132917	1.118175	1	1.740962	1.420567	-0.804124
1	-1.740300	1.548974	-0.599033	1	1.753616	1.281851	0.959088
7	-2.361412	-0.429894	-0.175387	7	2.349578	-0.463107	-0.069278
7	-3.573614	-0.261447	-0.057076	7	3.559005	-0.265404	-0.016970
7	-4.700903	-0.222157	0.017324	7	4.679179	-0.193404	0.020180

B3LYP/6-311+G(2d,p)

$\tilde{\nu} / \text{cm}^{-1}$	I / km mol ⁻¹	$\tilde{\nu} / \text{cm}^{-1}$	I / km mol ⁻¹
3108.6	0.0	950.5	0.2
3107.1	1.0	942.0	13.3
3077.2	0.1	924.4	1.2
3045.5	4.4	859.4	4.6
2899.2	16.5	832.1	48.6
2866.9	22.5	815.5	3.4
2173.0	745.4	796.8	7.6
1633.7	15.3	696.1	3.7
1535.7	7.4	663.9	3.6
1486.9	131.1	633.7	20.7
1456.6	11.6	565.5	5.2
1449.7	17.9	541.5	13.5
1351.2	85.9	510.6	13.8
1305.9	91.7	473.0	7.3
1298.6	24.0	418.1	0.2
1290.1	447.1	330.6	1.9
1227.2	2.4	301.1	8.7
1219.0	4.3	228.4	1.8
1194.0	2.6	133.4	1.2
1171.7	65.7	97.9	3.2
1099.8	3.2	32.1	0.3
1027.5	16.0	18.2	7.2
979.7	1.3		

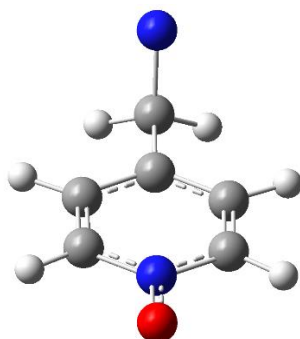
Transition state interconnecting **1g** and **1t**, TS (**1g-1t**)



B3LYP/6-311+G(2d,p)

6	6.000000	2.117474	1.043582
6	6.000000	0.805993	1.354276
6	6.000000	-0.100470	0.369538
6	6.000000	0.388610	-0.934645
6	6.000000	1.703163	-1.221093
1	1.000000	2.865741	1.759717
1	1.000000	0.495165	2.388363
1	1.000000	-0.257965	-1.753006
1	1.000000	2.142214	-2.205751
7	7.000000	2.578774	-0.240141
8	8.000000	3.797050	-0.517928
6	6.000000	-1.540418	0.693317
1	1.000000	-1.916431	0.074209
1	1.000000	-1.636487	1.739658
7	7.000000	-2.382389	0.502885
7	7.000000	-3.369533	-0.215713
7	7.000000	-4.300386	-0.859835

4-nitrenemethyl-pyridine-*N*-oxide (triplet) ³2



B3LYP/6-311+G(2d,p)

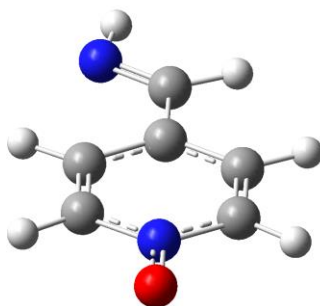
ω B97XD/6 311+G(2d,p)

6	-0.136983	-1.083869	1.174413	6	1.090446	-1.168922	-0.014349
6	-0.136983	0.292963	1.187782	6	-0.275099	-1.183401	-0.170726
6	-0.145165	1.023041	0.000000	6	-0.995073	0.001128	-0.259092
6	-0.136983	0.292963	-1.187782	6	-0.273998	1.184819	-0.169064
6	-0.136983	-1.083869	-1.174413	6	1.091571	1.168826	-0.012728
1	-0.138204	-1.705579	2.056581	1	1.709560	-2.050429	0.055513
1	-0.133206	0.795100	2.147583	1	-0.775317	-2.142827	-0.224577
1	-0.133206	0.795100	-2.147583	1	-0.773285	2.144804	-0.221569
1	-0.138204	-1.705579	-2.056581	1	1.711507	2.049659	0.058345
7	-0.138460	-1.784586	0.000000	7	1.781728	-0.000417	0.064084
8	-0.144643	-3.061602	0.000000	8	3.043410	-0.001130	0.202966
6	-0.102565	2.538249	0.000000	6	-2.502181	0.001769	-0.387846
1	-0.622617	2.939816	-0.884054	1	-2.841017	0.888393	-0.944747
1	-0.622617	2.939816	0.884054	1	-2.841204	-0.880420	-0.951663
7	1.241199	3.007053	0.000000	7	-3.117660	-0.003219	0.891317

B3LYP/6-311+G(2d,p)

$\tilde{\nu} / \text{cm}^{-1}$	I / km mol ⁻¹	$\tilde{\nu} / \text{cm}^{-1}$	I / km mol ⁻¹
3108.7	0.1	995.6	7.1
3107.5	1.0	945.6	0.0
3055.4	1.0	933.4	0.4
3055.2	3.6	854.8	1.9
2854.0	7.3	853.4	3.7
2824.5	15.3	843.0	42.4
1626.3	36.6	813.4	0.0
1533.2	0.5	762.3	10.6
1482.1	125.1	716.8	5.4
1452.4	5.2	659.8	0.2
1395.8	11.3	547.9	27.6
1314.6	0.4	483.0	11.7
1297.9	252.7	477.7	5.5
1250.3	2.5	418.0	0.0
1223.9	1.2	375.7	4.1
1189.6	6.1	292.4	0.1
1172.5	53.6	213.7	4.4
1121.1	6.4	101.1	5.1
1078.0	0.2	34.6	7.9
1027.1	21.4		

4-iminomethyl-pyridine-*N*-oxide (singlet), isomer **3E**



B3LYP/6-311+G(2d,p)

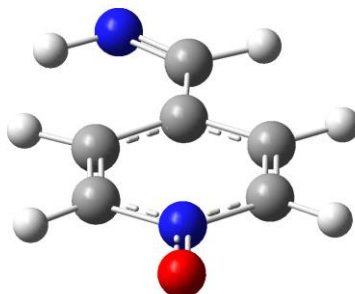
ω B97XD/6 311+G(2d,p)

6	-0.934653	-1.226520	0.000000	6	-0.980741	-1.183108	0.000010
6	-1.105527	0.133223	0.000000	6	0.380838	-1.041305	0.000006
6	0.000000	0.993726	0.000000	6	0.960983	0.226736	0.000047
6	1.264110	0.401659	0.000000	6	0.102900	1.319370	0.000005
6	1.407666	-0.967282	0.000000	6	-1.260975	1.145313	0.000020
1	-1.736652	-1.948826	0.000000	1	-1.502033	-2.128418	-0.000047
1	-2.105253	0.546930	0.000000	1	1.011687	-1.920822	-0.000018
1	2.159615	1.012089	0.000000	1	0.492281	2.330958	-0.000026
1	2.352929	-1.487840	0.000000	1	-1.984546	1.946199	-0.000032
7	0.317395	-1.791761	0.000000	7	-1.810520	-0.098093	0.000129
8	0.455603	-3.058438	0.000000	8	-3.067210	-0.250990	-0.000139
6	-0.148831	2.452167	0.000000	6	2.418791	0.411967	0.000073
1	0.794646	3.012058	0.000000	1	2.754705	1.456261	-0.000104
7	-1.289531	3.017259	0.000000	7	3.217461	-0.571783	-0.000045
1	-1.201746	4.032776	0.000000	1	4.186221	-0.260961	-0.000210

B3LYP/6-311+G(2d,p)

$\tilde{\nu} / \text{cm}^{-1}$	I / km mol ⁻¹	$\tilde{\nu} / \text{cm}^{-1}$	I / km mol ⁻¹
3340.2	10.2	1021.2	20.3
3109.0	0.0	967.7	0.8
3107.4	1.0	938.7	1.6
3075.4	1.3	862.5	80.4
3049.6	3.5	853.7	11.3
2891.6	52.1	818.0	2.8
1645.4	65.7	790.2	2.3
1623.2	177.7	777.5	3.6
1529.0	19.4	688.7	1.6
1485.1	80.5	659.7	3.1
1452.9	36.0	595.7	63.0
1395.0	18.5	507.6	27.0
1311.2	72.2	474.2	16.5
1306.8	207.9	421.1	1.0
1241.3	30.4	403.4	3.3
1217.7	12.5	307.7	32.2
1174.1	13.9	202.4	6.6
1142.2	178.4	164.1	4.2
1093.9	10.0	90.0	8.9
1068.0	3.0		

4-iminomethyl-pyridine-*N*-oxide (singlet), isomer **3Z**



B3LYP/6-311+G(2d,p)

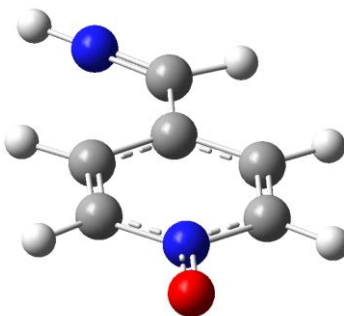
ω B97XD/6-311+G(2d,p)

6	-0.948093	-1.219411	0.000000	6	0.987734	-1.181210	0.000044
6	-1.106746	0.142958	0.000000	6	-0.375590	-1.046343	0.000017
6	0.000000	1.000479	0.000000	6	-0.971102	0.213821	0.000042
6	1.258347	0.392015	0.000000	6	-0.113620	1.309249	-0.000016
6	1.393384	-0.976752	0.000000	6	1.250565	1.146484	0.000012
1	-1.757757	-1.933043	0.000000	1	1.512289	-2.124676	-0.000013
1	-2.117554	0.532267	0.000000	1	-0.970016	-1.952091	-0.000015
1	2.157532	0.996683	0.000000	1	-0.510620	2.317636	-0.000082
1	2.335585	-1.503034	0.000000	1	1.967272	1.953633	-0.000074
7	0.297623	-1.795072	0.000000	7	1.810856	-0.092856	0.000202
8	0.425543	-3.061756	0.000000	8	3.067300	-0.237684	-0.000170
6	-0.100127	2.470763	0.000000	6	-2.432399	0.430960	0.000024
1	0.865288	2.984243	0.000000	1	-2.730885	1.482834	0.000051
7	-1.135714	3.208475	0.000000	7	-3.364084	-0.425836	-0.000072
1	-2.001390	2.662798	0.000000	1	-3.007362	-1.382785	-0.000143

B3LYP/6-311+G(2d,p)

$\tilde{\nu} / \text{cm}^{-1}$	I / km mol ⁻¹	$\tilde{\nu} / \text{cm}^{-1}$	I / km mol ⁻¹
3340.2	10.2	967.7	0.8
3109.0	0.0	938.7	1.6
3107.4	1.0	862.5	80.4
3075.4	1.3	853.7	11.3
3049.6	3.5	818.0	2.8
2891.6	52.1	790.2	2.3
1645.4	65.7	777.5	3.6
1623.2	177.7	688.7	1.6
1529.0	19.4	659.7	3.1
1485.1	80.5	595.7	63.0
1452.9	36.0	507.6	27.0
1395.0	18.5	474.2	16.5
1311.2	72.2	421.1	1.0
1306.8	207.9	403.4	3.3
1241.3	30.4	307.7	32.2
1217.7	12.5	202.4	6.6
1174.1	13.9	164.1	4.2
1142.2	178.4	90.0	8.9
1093.9	10.0		
1068.0	3.0		

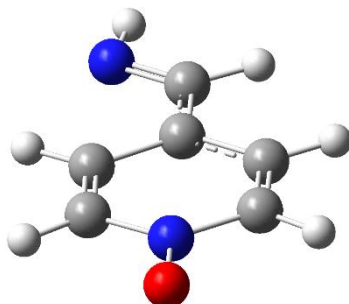
Transition state interconnecting **3E** and **3Z**, TS (**EZ**)



ω B97XD/6-311+G(2d,p)

6	-0.975743	-1.187419	0.000017
6	0.385055	-1.032042	0.000021
6	0.954326	0.237232	0.000004
6	0.089224	1.323035	-0.000017
6	-1.273243	1.138988	-0.000021
1	-1.490234	-2.136522	0.000030
1	1.023919	-1.906846	0.000036
1	0.475515	2.336304	-0.000030
1	-2.004122	1.933354	-0.000038
7	-1.813187	-0.109060	-0.000004
8	-3.069160	-0.271752	-0.000007
6	2.427964	0.443027	0.000006
1	2.708675	1.515284	0.000014
7	3.277558	-0.451235	0.000001
1	3.943437	-1.182418	-0.000003

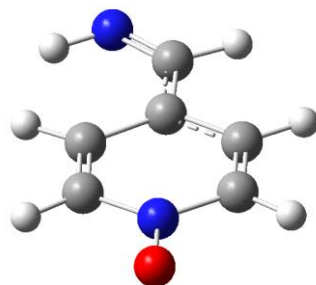
4-iminomethyl-pyridine-*N*-oxide (triplet), isomer **³E**



ω B97XD/6-311+G(2d,p)

6	0.938949	-1.231053	0.000000
6	-0.386576	-1.077421	0.000007
6	-0.978993	0.251384	0.000010
6	-0.069651	1.373935	-0.000002
6	1.254433	1.188890	-0.000009
1	1.462692	-2.175727	-0.000002
1	-1.041397	-1.937226	0.000012
1	-0.460721	2.383878	-0.000005
1	2.002121	1.967764	-0.000018
7	1.790430	-0.114348	-0.000004
8	3.060932	-0.272537	-0.000059
6	-2.380000	0.431158	0.000023
1	-2.734449	1.467343	0.000029
7	-3.193911	-0.583131	0.000037
1	-4.160304	-0.264732	0.000051

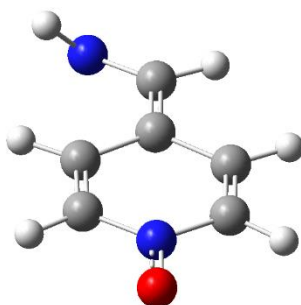
4-iminomethyl-pyridine-*N*-oxide (triplet), isomer **³Z**



ω B97XD/6-311+G(2d,p)

6	-0.950909	-1.227585	0.000016
6	0.376579	-1.086322	0.000000
6	0.990623	0.233983	-0.000001
6	0.083907	1.361101	-0.000001
6	-1.241702	1.192997	0.000017
1	-1.480296	-2.169138	0.000015
1	0.987225	-1.979013	-0.000011
1	0.486381	2.366401	-0.000013
1	-1.980279	1.980404	0.000019
7	-1.792061	-0.106326	0.000037
8	-3.063567	-0.256083	-0.000074
6	2.393578	0.445354	0.000002
1	2.708992	1.490773	0.000015
7	3.348392	-0.432727	0.000014
1	2.979745	-1.384564	0.000017

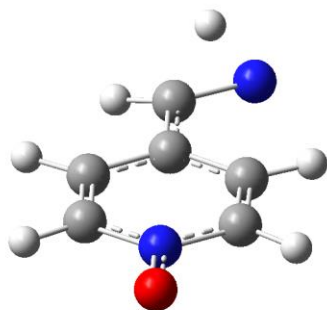
Transition state interconnecting ³E and ³Z, TS (³EZ)



ω B97XD/6-311+G(2d,p)

6	0.932269	-1.205303	-0.008305
6	-0.404152	-1.048107	0.002677
6	-1.003991	0.270248	0.024120
6	-0.064561	1.371567	0.008460
6	1.261243	1.161297	0.001401
1	1.439301	-2.159075	-0.016779
1	-1.027879	-1.932148	-0.010013
1	-0.433652	2.389409	0.009961
1	2.011031	1.938497	0.001371
7	1.791122	-0.122096	-0.007864
8	3.050920	-0.296329	-0.004672
6	-2.348995	0.480408	0.028628
1	-2.724431	1.501600	-0.012402
7	-3.316221	-0.496336	-0.117700
1	-3.226914	-1.219283	0.602301

Transition state interconnecting ${}^3\mathbf{3E}$ and ${}^3\mathbf{2}$, TS (${}^3\mathbf{HT}$)



$\omega\text{B97XD/6-311+G(2d,p)}$

6	-0.964539	-1.183183	-0.005668
6	0.396580	-1.033075	-0.014345
6	0.977212	0.243829	-0.013841
6	0.095008	1.333880	-0.009261
6	-1.259014	1.142279	-0.001450
1	-1.473035	-2.135619	-0.011111
1	1.016356	-1.920665	-0.030151
1	0.470903	2.349786	-0.013279
1	-1.989304	1.937341	-0.001459
7	-1.803609	-0.109459	0.003950
8	-3.064318	-0.267997	0.013070
6	2.407068	0.441761	0.008136
1	2.805111	1.411799	-0.293512
1	3.053180	-0.006403	1.005313
7	3.334672	-0.628428	-0.081347